Precessional Frequency Tuning in $Ni_{81}Fe_{19}/(Ni_{81}Fe_{19})_{1-x}Eu_x$ (50 nm) Bilayers

Lili Cheng, Hajung Song, and William E. Bailey

***Abstract*—We present a study of the precessional dynamics of exchange coupled $Ni_{81}Fe_{19}/Ni_{81}Fe_{19}$:$Eu_x$ bilayers, 50 nm thick. Eu codopants are of interest in soft ferromagnetic films since they can be used to enhance the gigahertz precessional frequency (f_p) in $Ni_{81}Fe_{19}$ thin films without contributing to damping. Underdamped precessional dynamics with f_p "tunable" by as much as roughly 0.3 GHz were observed. Dynamical behavior agrees well with a single-domain Landau–Lifshitz simulation at constant relaxation rate $\lambda/4\pi = 150$ MHz across the series. The variation of precessional frequency with bias field shows that the enhancement of resonant frequency arises from an increase of dynamic anisotropy H_K, matched well by static H_K as measured by SQUID. An increasing contribution in g factor (2.1–2.4) is mostly balanced by a decreasing saturation magnetization M_s.**

***Index Terms*—Bilayers, Eu, magnetization dynamics, $Ni_{81}Fe_{19}$.**

I. Introduction

AS DATA RATES in magnetic information storage approach 1 GHz and above, strategies to control the magnetization dynamics in thin films become a more pressing need. While some recent work has proposed control through precise timing of magnetic field pulses [1], [2], materials-based strategies can offer a more straightforward implementation. We have proposed that dilute concentrations of rare-earth elements can be used to tune the dynamic response of ferromagnetic thin-film magnetization [3]. A systematic variation in strength has been observed across the lanthanide series [4]. Among these elements, Eu is special in that it does not contribute damping to the system, but increases the precessional frequency by roughly 0.1 GHz per atomic percentage. The dopants can thus be used to raise a basic speed limit to precessional motion.

We examined the effect of Eu-doped thickness fraction on the precessional frequency of $Ni_{81}Fe_{19}/Ni_{81}Fe_{19}$:$Eu_x$ bilayers. The Eu-doped $Ni_{81}Fe_{19}$ is a high f_p layer and $Ni_{81}Fe_{19}$ is a lower f_p layer; bilayers exhibited intermediate values. This bilayer structure could be useful in magnetoelectronics such as GMR spin valves. Our motivation is to remove dopants which control dynamics from ferromagnetic/nonmagnetic interfaces which control spin transport. We present a study of the dynamic properties including relaxation rate λ, precessional frequency f_p, spectroscopic splitting factor g, as well as static magnetic properties of the bilayer, as a function of Eu-doped thickness fraction.

Manuscript received January 28, 2004. This work was supported by the Army Research Office Young Investigation Program (ARO-43986-MS-YIP) and NIST Nanomagnetodynamics (60NANB2D0145). The work has used the shared experimental facilities that are supported primarily by the MRSEC Program of the National Science Foundation under Award Number DMR-0213574. The work of H. Song was supported in part by a Korean Science and Engineering Foundation (KOSEF) fellowship.

The authors are with the Materials Science Program, Department of Applied Physics, Columbia University, New York, NY 10027 USA (e-mail: lc665@columbia.edu; web54@columbia.edu; hjsong@hotmail.com).

Digital Object Identifier 10.1109/TMAG.2004.832260

II. Experimental Method

The bilayer structure $SiO_2/Ni_{81}Fe_{19}([1 - y]50$ nm$)/$ $Ni_{81}Fe_{19}$:$Eu_x([y]50$ nm$)/$Ta was prepared by ion-beam sputtering. Eu dopants were introduced by cosputtering with a Eu thin foil, mounted to a Cu block, positioned in front of the $Ni_{81}Fe_{19}$ target by a manipulator arm with motion feedthrough. The Eu content in Eu-doped layer was fixed at $x = 3\%$. The total bilayer thickness is 50 nm. The thickness fraction y of the Eu-doped region varied as $0 \le y \le 1$. Uniaxial anisotropy was induced by application of a magnetic field (~20 Oe) during deposition.

Magnetization dynamics of the bilayer were investigated at 10–20 GHz bandwidth by time-domain pulsed inductive microwave measurement (PIMM) with step pulse field excitation [5]. In this technique, a step current pulse is delivered to the coplanar waveguide, generating a pulsed Biot–Savart field in a magnetic thin film placed on top of the waveguide. The pulse width is 10 ns and the measured risetime is <100 ps. A static bias field, variable from 0 to 30 Oe, was applied in the easy axis direction, transverse to the pulse field direction. For a thin film under the combination of the two fields in the film plane, the magnetization angle will evolve as an exponentially decaying sinusoidal function

$$\phi(t) = \phi_0 + \beta_0 \sin(\omega_p t + \varphi) e^{-\lambda t/2} \tag{1}$$

in which ϕ_0 is the equilibrium angle canted from the easy axis, parallel to the vector sum of pulse, anisotropy, and bias field, and ω_p is the precessional angular frequency [5]. The detected inductive voltage is proportional to dM_y/dt, where M_y is the component of magnetization M in the direction of the hard axis, and is proportional to $d\phi(t)/dt$ for small displacement angles. Dynamic measurement data were fitted to the numerically integrated Landau–Lifshitz (LL) equation. Fit parameters, including the anisotropy field H_k, the relaxation rate λ, and the spectroscopic splitting factor g were extracted as a function of thickness fraction y. Static magnetic properties were measured by superconducting quantum interference device (SQUID) magnetometry.

III. Experimental Results

A. Magnetization Dynamics

Fig. 1 shows inductive waveforms of $Ni_{81}Fe_{19}/$ $(Ni_{81}Fe_{19})_{1-x}Eu_x$ bilayers with 5 Oe bias field. As the thickness fraction of the Eu-doped layer y increases, we see

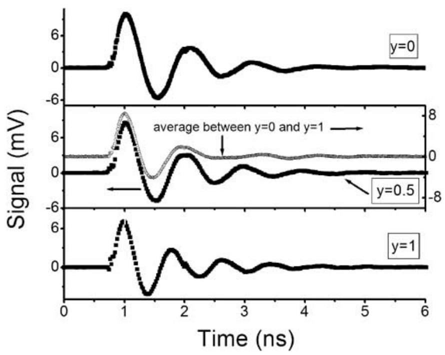

Fig. 1. Inductive waveforms of $Ni_{81}Fe_{19}([1-y]50$ nm)/ $Ni_{81}Fe_{19}$: $Eu_x([y]50$ nm) bilayers, acquired with 5 Oe of transverse bias. Average from $y=0$ and $y=1$ is also shown for comparison.

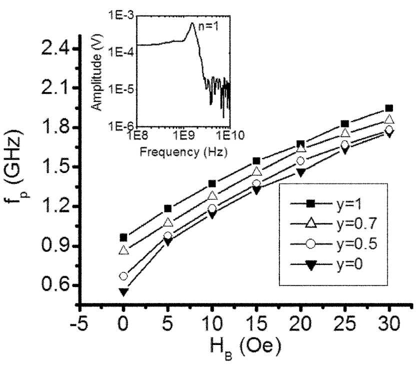

Fig. 2. Precessional frequency f_p versus bias field H_B of $Ni_{81}Fe_{19}([1-y]50$ nm)/ $Ni_{81}Fe_{19}$:$Eu_x([y]50$ nm) bilayers, thickness fraction $0 \leq y \leq 1$. Inset shows Fourier transformation of data for $y=0.5$ with $H_B = 20$ Oe.

more oscillations in the waveform over a fixed period of time, indicating higher precessional frequency. The full width at half maximum (FWHM) of the primary inductive wave is 250 ps for $y=1$, as compared with 330 ps for $y=0.5$ and 350 ps for $y=0$. We performed a simple average between the signals for $y=1$ and $y=0$, and the result is also shown in Fig. 1, which is quite different from $y=0.5$. We can see that the response from bilayers is not simply the superposition of the two single layers. This illustrates the strong exchange coupling between the two layers. Similar measurements were completed with increasing dc bias fields applied along the easy-axis direction.

The time-domain data were transformed to the frequency domain by fast Fourier transform, as shown in the inset of Fig. 2. The frequency of the lowest spectral peak $(n=1)$ is almost the same as that extracted from the sinusoidal fitting. This frequency is believed to approach the standard FMR result for weak damping [5], [6] and was studied here. Fig. 2 shows the extracted precessional frequency f_p as function of bias field H_B for the bilayers with different thickness fraction y. For the series studied, the precessional frequency has been increased by as much as roughly 0.3 GHz across the series in the bilayers.

Magnetization dynamics measurements were fitted to both exponentially decaying sinusoidal function and the numerically integrated full-angle LL equation for relaxation rate λ. Both methods give similar results. Fig. 3 shows the extracted relaxation rate λ at $H_B = 20$ Oe as a function of thickness fraction. By both methods, as thickness fraction y changes from 0 to 1, there is no significant change in the damping parameter. The relaxation rate $\lambda/4\pi$ remains ~150 MHz for LL simulation and ~140 MHz

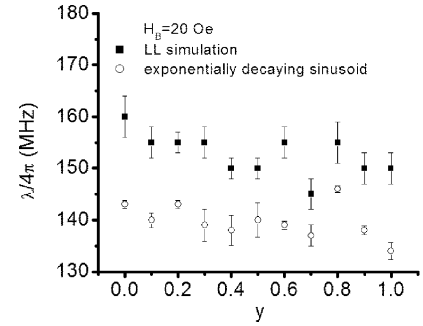

Fig. 3. Relaxation rate λ of bilayers, simulated from both exponentially decaying sinusoid and numerically integrated LL equation.

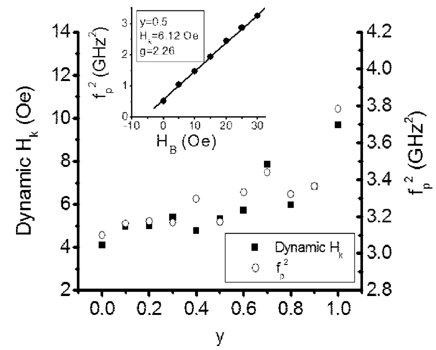

Fig. 4. Dynamic anisotropy field H_k of the bilayers, extracted from the interception with H_B in Kittel plot. The corresponding f_p^2 for $H_B = 20$ Oe is also shown for comparison. The inset is the Kittel plot for $y = 0.5$.

for sinusoidal function. The same analysis was also applied to different dc bias fields and consistent results were found.

The Kittel equation describes ferromagnetic resonance for a thin film magnetized in plane [7]:

$$f_p = \left(\frac{\gamma\mu_0}{2\pi}\right) Ms^{1/2}(H_K + H_B)^{1/2} \tag{2}$$

in which

$$\gamma = g\frac{\mu_B}{\hbar} \tag{3}$$

where μ_B is the Bohr magneton and $\hbar$ is Planck's constant $h/2\pi$ $(= 1.05 \times 10–34$ J $\cdot$ s). From (2) and (3), plotted as f_p^2 versus H_B, we can extract both g factor and dynamic anisotropy field H_K. Fig. 4 shows the dynamic H_K as function of thickness fraction y. The inset shows the linear relationship between f_p^2 and H_B for the sample with thickness fraction $y = 0.5$. g factor was extracted as 2.26 from the slope and dynamic H_k 6.12 Oe from the interception with H_B. As the thickness fraction of the Eu-doped layer increases, dynamic H_k also increases. The corresponding f_p^2 is shown in the figure for comparison.

We find that the boost of precessional frequency from Eu dopants corresponds well to an enhancement of anisotropy. Present results suggest an identity between dynamic and static anisotropy field (see below).

g factors extracted from both LL simulation and Kittel plot are shown in Fig. 5. In both methods, the g factor changes linearly as the thickness fraction of Eu-doped layer increases. g factor values measured by fp(HB) fits, taking the FFT-derived values of fp, yield g-factor values increasing from 2.0 to 2.3. Estimates taken by the full LLG fit are ~0.1 higher, due in part to some deviation from the simulation at longer times. The measured values for undoped Ni_81Fe_19 of 2.0 and 2.1 are close to

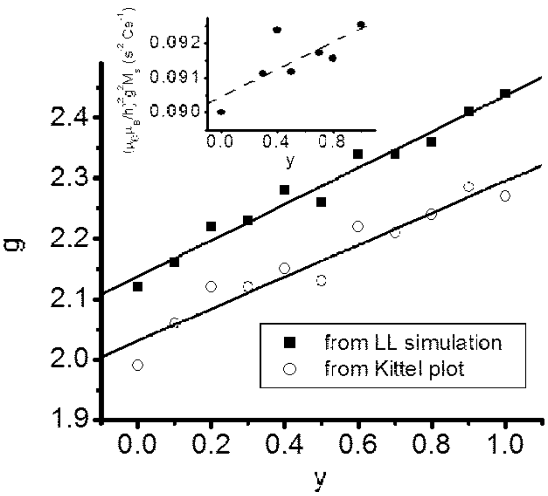

Fig. 5. g factor of bilayers, extracted from LL simulation and Kittel plot separately. Inset: slope in Kittel plot, $(\mu_0\mu_B/h)^2g^2$ Ms, versus thickness ratio y.

the $g = 2.05$ measured by Silva *et al.* The inset in Fig. 5 shows the slope of Kittel plot, $(\mu_0\mu_B/h)^2g^2M_s$, versus thickness ratio y. As y increases, there is a slight increase in the slope, about 2% more for $y = 1$ than for $y = 0$. As later we will show that magnetization M_s decreases with y, this result indicates that the increasing rate of g^2 is slightly faster than the decreasing rate of M_s. Since g is directly related to the ratio of orbital and spin moment [8], [9]

$$\frac{\mu_L}{\mu_S} = \frac{g}{2} - 1 \tag{4}$$

the increase of g across the series suggests that fraction of the total momentum contributed by orbital motion compared with that contributed by spin motion is strengthened as the Eu-doped layer thickness is increased. However, at present, we have not been able to verify this by X-ray magnetic circular dichroism (XMCD); Fe edges of the $Ni_{81}Fe_{19}$ show μ_L/μ_S ratios which are constant and independent of Eu doping, and only negligible XMCD signals have been observed on Eu [10].

B. Static Magnetic Properties

The easy and hard axis hysteresis loops were measured by SQUID magnetometry for the whole series. Shown in Fig. 6(a) are those for $y = 1$ (Eu-doped $Ni_{81}Fe_{19}$ single film) and $y = 0$ ($Ni_{81}Fe_{19}$ single film). For the series tested, the squareness along the easy axis is very well defined. As thickness fraction of Eu doped layer increases from 0 to 1, coercivity H_c increases from 1.2 to 2.8 Oe, and anisotropy field H_k increases from 2.7 to 11.6 Oe. The static anisotropy field agrees well with the dynamic value. This observation disagrees with previous finding that dynamic H_k is larger than the static value in Eu-doped $Ni_{81}Fe_{19}$ thin films (measured by magneto-optical Kerr effect) (as in [3]); we presume that the improved resolution of the SQUID has given more reliable data.

Saturation magnetization Ms was calculated from the magnetic moment measured by SQUID. The volume of the measured sample was measured through a combination of profilometric film thickness and the mass of the film plus substrate. Fig. 6(b) shows Ms as function of y. As y increases, Ms decreases. This is consistent with previous data for Gd and Tb doped films and the idea that RE moments align antiparallel with transition metal moments (as in [4]).

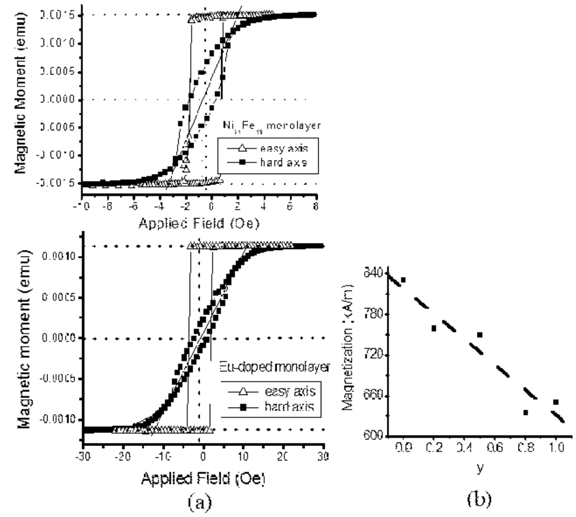

Fig. 6. Static magnetic properties measured by SQUID at room temperature. (a) Easy-axis and hard-axis hysterysis loops for $Ni_{81}Fe_{19}$ and Eu-doped $Ni_{81}Fe_{19}$ (50 nm) single films, separately. Note the scale change of applied field. (b) Saturation magnetization of the bilayers.

IV. Conclusion

A bilayer method was demonstrated to tune the precessional frequency in $Ni_{81}Fe_{19}$ thin films with minimal effect on the damping parameter. The measured dynamic data were fitted to both the Landau–Lifshitz equation and exponentially decaying sinusoid and the extracted parameters agree well with each other. Strongly enhanced anisotropy in the films (2.7 to 11.6 Oe) is important to explain the boost in the resonance frequency (of 300 MHz).

References

[1] T. M. Crawford, P. Kabos, and T. J. Silva, "Coherent control of precessional dynamics in thin film permalloy," *Appl. Phys. Lett.*, vol. 76, pp. 2113–2115, Apr. 2000.

[2] T. Gerrits, H. A. M. van den Berg, J. Hohlfeld, O. Gielkens, L. Bär, and T. Rasing, "Picosecond control of coherent manetization dynamics in permalloy thin films by picosecond magnetic field pulse shaping," *J. Magn. Magn. Mater.*, vol. 240, pp. 283–286, 2002.

[3] W. Bailey, P. Kabos, F. Mancoff, and S. Russek, "Control of magnetization dynamics in $Ni_{81}Fe_{19}$ thin films through the use of rare-earth dopants," *IEEE Trans. Magn.*, vol. 37, pp. 1749–1754, July 2001.

[4] S. G. Reidy, L. Cheng, and W. E. Bailey, "Dopants for independent control of precessional frequency and damping in $Ni_{81}Fe_{19}$ (50 nm) thin films," *Appl. Phys. Lett.*, vol. 82, pp. 1254–1256, Feb. 2003.

[5] T. Silva, C. Lee, T. Crawford, and C. Rogers, "Inductive measurement of ultrafast magnetization dynamics in thin-film permalloy," *J. Appl. Phys.*, vol. 85, pp. 7849–7862, June 1999.

[6] D. O. Smith, "Magnetization reversal and thin films," *J. Appl. Phys.*, vol. 29, pp. 264–273, Mar. 1958.

[7] C. Kittel, *Introduction to Solid State Physics*, 6th ed. New York: Wiley, ch. 1986, pp. 481–481.

[8] F. Schreiber, J. Pflaum, Z. Frait, T. Mühge, and J. Pelzl, "Gilbert damping and g-factor in Fe_xCo_{1-x} alloy films," *Solid State Commun.*, vol. 93, pp. 965–968, 1995.

[9] M. Blume, S. Geschwind, and Y. Yafet, "Generalized Kittel-Van Vleck relation between g and g': Validity for negative g factors," *Phys. Rev.*, vol. 181, pp. 478–487, May 1969.

[10] W. E. Bailey, H. Song, and L. Cheng, "Fe orbital moment in lanthanide doped $Ni_{81}Fe_{19}$," *J. Appl. Phys.*, to be published.